

# RESONANCE TRAPPING, STOCHASTIC DIFFUSION AND INCOHERENT EMITTANCE GROWTH INDUCED BY STRUCTURED ELECTRON-CLOUD PINCH

G. Franchetti, GSI Darmstadt, Germany; F. Zimmermann, CERN Geneva, Switzerland

## Abstract

When a bunch passes through an electron cloud, the transverse electron density distribution is enhanced and modulated in time as a consequence of the motion of individual electrons under the action of the nonlinear beam field. The effect of this “structured” electron pinch together with the synchrotron motion of beam particles leads to an incoherent emittance growth via the excitation and repeated crossing of resonances, that can give rise to either stochastic “scattering” (“diffusion”) or trapping. We study these effects via a toy model of an idealized pinch, and present applications to the CERN SPS and the GSI SIS100.

## LANDSCAPE

It is well known that the excitation of nonlinear resonances by magnet errors, space charge or beam-beam interaction in conjunction with tune modulation can lead to stochastic diffusion, resonance trapping and emittance growth in hadron storage rings. Already in the 1950s the change of a particle’s oscillation amplitude due to a single “fast” resonance crossing was calculated by Schoch [1] following earlier work by mathematicians. In the 1970s A. Chao and M. Month stressed the complementary possibility of adiabatically trapping particles in resonance islands, and transporting them, via a slow tune modulation, towards larger amplitudes [2]. Since the times of Schoch, Month or Chao, several novel theoretical approaches for describing the effect of tune modulation have been developed in the field of nonlinear dynamics, e.g., a theory of “modulational diffusion” by Chirikov, Vivaldi, Lieberman and co-workers [3]. Following the above pioneers, over many decades numerous theoretical and experimental studies were conducted on the combined effects of tune modulation and nonlinear forces in accelerators. A review of these phenomena in regard to beam-beam interaction, including estimates of diffusion rates, was delivered by L. Evans in a school for the SPS collider [4]. A review of related diffusion mechanisms in regard to nonlinear magnetic field errors was also published more than 10 years ago [5]. An extrapolation of the dynamic aperture due to field errors in the presence of tune modulation was derived by a Bologna-CERN collaboration [6]. Later, the interplay of direct space charge and tune modulation was studied for the LHC [7]. In 1999 M.A. Furman and A.A. Zholents pointed out, for the first time, that the “pinch” of an electron cloud during a bunch passage induces a tune shift changing along the bunch, which together with synchrotron motion excites synchro-betatron resonances [8]. The phe-

nomenon considered was found not to be a strong effect for the PEP-II B factory. At about the same time, K. Oide also hypothesized about an incoherent electron-cloud effect, as a possible explanation for the vertical beam-size blow up that was observed at the KEKB positron ring. The KEKB beam blow up was however soon explained in theory and simulations by a TMC-like fast head-tail instability [9], an explanation which was afterwards confirmed experimentally [10]. Nevertheless some KEKB data suggest that even below the threshold of the fast instability a small “incoherent” blow up occurs [11]. The detailed distribution of the pinched electron cloud inside a KEKB positron bunch and the resulting large incoherent tune shift, computed in 2000 [12], suggest a possible explanation. In 2001 the incoherent tune shift due to an electron cloud at the end of a bunch passage was also estimated for the LHC proton beam in the PS, SPS and LHC [13]. An analytical few-particle model, including the tune shift from space charge and from electron cloud (with a simplified “linear” pinch), plus synchrotron motion, was developed by G. Rumolo *et al.* [14], following a suggestion by K. Cornelis. In a 2002 memorandum K. Ohmi discussed the incoherent electron-cloud effect, emphasizing its similarity to the incoherent effect of space charge [15]. He later compared this effect with a linear stopband resonance due to a quadrupole error [16]. In 2003, the tune footprint created by the pinched electron cloud was calculated via frequency maps, revealing several resonances which would potentially contribute to an incoherent emittance growth [17]. Accompanying longer-term tracking simulations showed a strong dependence of the emittance growth on the synchrotron tune. Also, in 2004, E. Benedetto *et al.* presented an analytical calculation of the electron-induced incoherent tune shift as a function of the longitudinal and transverse beam-particle position along the bunch, assuming that this tune shift could be responsible for incoherent emittance growth [18, 19]. Incoherent space-charge effects in high-intensity high-brightness beams have become more relevant with the advent of new projects such as FAIR [20]. In preparation of FAIR, these effects have been studied in an extensive experimental campaign at CERN [21], which was accompanied by several numerical benchmarking studies [22]. The main outcome of this campaign is that a particle may indeed be trapped in a resonance when the latter is crossed, as predicted by Chao and Month more than 30 years earlier. The resonance crossing and trapping is particularly relevant in bunched beams where particles, due to space charge, may periodically be subjected to a resonance crossing via the synchrotron motion.

In September 2004 some analogies were drawn between resonance-trapping phenomena for space charge invoked to explain the beam losses observed during the PS measurement campaign, and beam losses seen at the SPS, which could be due to space charge or electron cloud, during discussions at CERN by E. Metral, E. Shaposhnikova, and G. Arduini, in connection with the ICFA-HB2004 workshop [23]. Inspired by the remarkable similarities of incoherent space charge effects and incoherent electron cloud effects, that had already been exploited by G. Rumolo *et al.* [14] and by K. Ohmi [15], the CARE-HHH 2004 workshop established a close collaboration between CERN, GSI, and KEK [24], which culminated in the use of an analytical electron-pinch model all around the ring for detailed long-term tracking studies of the SPS and LHC [25], and in an alternative description and interpretation put forward by K. Ohmi and K. Oide, who refer to it as “6-dimensional Arnold diffusion” [26]. The pinching of the electron cloud, either in a field-free region or in magnetic field, leads to a complicated structure with a series of higher density regions, which are successively emerging on the beam axis, at various longitudinal positions along the bunch. The regions of peak density are a result of the transverse oscillatory electron motion. After its formation on axis, each high-density region soon splits into two, on either side of the beam. During the later part of the bunch passage, the two newly generated electron “stripes” are then moving outward, away from the transverse bunch center. Such electron structures were first obtained from an analytical model of the pinch for a round beam without magnetic field [18, 19] and later reproduced in detailed pinch simulations with the HEADTAIL code [27] for various beam and magnetic field conditions [28]. The presence of an electron stripe and its transverse distance from the bunch center depends on the longitudinal coordinate  $z$  describing the longitudinal position along the bunch with respect to a co-moving reference particle. Therefore, there exists a correlation between the electron-cloud field experienced by a beam particle and its longitudinal position in the bunch. Via the synchrotron motion this dependence translates into a tune modulation, a mechanism that is familiar from space charge. In numerical simulations the long-term effect of a localized pinched electron cloud is a non-negligible emittance growth [24], which vanishes if the longitudinal motion of the particles in the bunch is artificially frozen [25]. Unfortunately a fully self consistent simulation of a bunched beam interacting with a pinching electron cloud all around a storage ring is prohibitively CPU time consuming, for typical storage times of a rings like the SPS or the LHC which range from 20 minutes to several hours in real time. As a remedy we may employ the simplifying assumption that the electron pinch identically repeats on each successive bunch passage through the same or equivalent location. However, even with this assumption the number of turns which can be explored is

relatively small [25]. In an attempt to overcome this difficulty and to unravel the mechanisms of the slow emittance growth, a further simplified analytical model of the pinched electron cloud was constructed based on the principle of electron charge conservation and assuming that the pinch increases linearly along the bunch. For the purpose of comparison, this simplified model was also implemented in the PIC code HEADTAIL and over 5000 turns and 10000 turns a simulation benchmarking has been performed [25]. Other benchmarking efforts were reported in Ref. [29]. However, up to now, in the “frozen models” of the electron cloud, the presence of the electron “stripes” was completely ignored. In this paper, we address the effect of the pinch structure on the beam dynamics. We adopt a simplified model in order to gain a first qualitative and semi-quantitative understanding of the role of the electron “stripes” on the beam dynamics.

## “STRIPES” PINCH MODEL

The pinch of the electron cloud gives rise to the formation of a certain number of “stripes” [18, 19]. The morphology of each electron stripe is quite complex, and the effect of the stripe on the beam dynamics is difficult to assess. We simplify the problem by considering idealized electron stripes formed mainly in the horizontal direction and extending infinitely in the vertical plane (Fig. 1). This simplification is a reasonable approximation for the

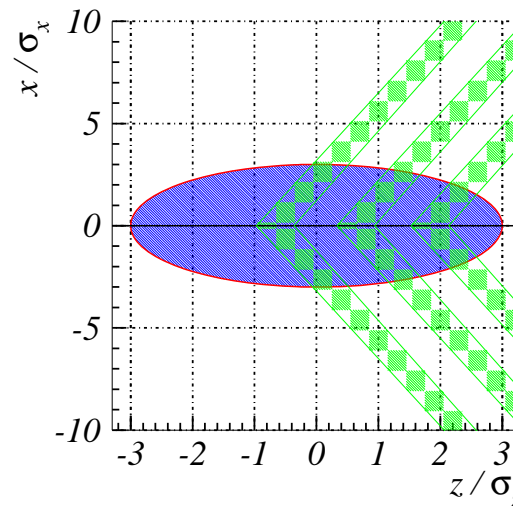


Figure 1: Schematic of a one-dimensional model of electron-cloud stripes in the bunch reference frame. Indicated in blue is the  $x - z$  area occupied by a bunch. The electron stripes are shown as green bands.

pinch occurring with a flat beam in a vertical magnetic field [28], and it allows for a straightforward analytical description of the electric field. The picture shows an example of three electron stripes modeled by straight walls of uniform electron density  $\rho_e$ . The change of the hori-

zonal stripe location with location  $z$  is taken to be small, i.e.  $\theta \equiv dx/dz|_{\text{stripe}} \ll 1$ . The electron density of our model is chosen as constant inside the stripes and zero outside, namely

$$\rho(x) = \begin{cases} 0 & \text{if } 0 < |x| < R_1 - \Delta R \\ \rho_e & \text{if } R_1 - \Delta R < |x| < R_1 \\ 0 & \text{if } R_1 < |x| \end{cases} \quad (1)$$

where  $\Delta R$  denotes the  $x$ -thickness of the stripe, and  $R_1$  is the outer horizontal border of the electron wall. In this approximation the electric field is readily computed via Gauss's law, and we find that the electric field is absent inside the stripes (i.e. for  $|x| < R_1 - \Delta R$ ), and constant outside the stripes (i.e. for  $|x| > R_1$ ). At each  $z$ , the total electric field  $E_x$  is the composition of the electric field produced by all individual electron stripes which are present. We denote by  $z_p$  the start position of a new pair of two stripes. In our model, electrons belonging to the same stripe are found on the bunch axis over the longitudinal region  $(z_p, z_p + \Delta R/\theta)$ . This short region correspond to a maximum of the pinch.

Consider a ring with a highly localized electron cloud described by a single interaction point (IP) between the electrons and the beam. In such case, the density  $\rho_e$  can be related to the detuning produced at the center of the pinch, via the relation

$$\Delta Q_{x,ec1} \approx \frac{\beta_{x,IP} e \rho_e q}{4\pi \epsilon_0 p_0 v_0} \Delta s, \quad (2)$$

where  $\beta_{x,IP}$  designates the beta function at the IP,  $\epsilon_0$  the vacuum permittivity,  $\rho_e$  the EC density within a stripe,  $q$  the charge of the beam particle,  $e$  the electron charge,  $p_0$  the beam particle's longitudinal momentum,  $v_0$  its longitudinal velocity, and  $\Delta s$  the longitudinal extent of the electron cloud. If many IPs are present in the ring and the detuning from each IP is small, then the global detuning is the sum of the individual detuning contributions from all IPs. If the detuning from the individual IPs is too strong (or the betatron tune close to an integer or half integer), higher order term enter into the evaluation of the total EC detuning. Note that Eq. (2) is valid only for particles experiencing linear electron forces at the location of the pinch. For particles at larger amplitudes (e.g.  $|x| > \Delta R$ ), or at different longitudinal locations (in the bunch reference frame) the expression for the detuning is more complicated. In the model of Fig. 1 each stripe intersects the axis at an angle  $\theta = 3.33\sigma_x/\sigma_z$ , the  $x$ -thickness of the stripe is  $\Delta R = 1\sigma_x$ , and the three stripes have their pinch maxima located at the positions  $z_p = -1\sigma_z, 0.3\sigma_z$ , and  $1.5\sigma_z$ , respectively.

## DETUNING AT LARGE AMPLITUDE

We consider the model of Fig. 1 where a single electron stripe produces a detuning of  $\Delta Q_{x,ec1} = 0.02$ . The density  $\rho_e$  is set via Eq. (2). We take a test particle at the longitudinal position of the pinch  $z = -0.9\sigma_z$  (in the bunch reference frame). If the linear oscillation amplitude of a par-

ticle is large, i.e.  $X \equiv \sqrt{2I_x/\beta_{x,IP}} \gg R_1$  (with  $I_x$  denoting the classical action variable, equal to half the Courant-Snyder invariant), the detuning is mainly determined by the effect of the electric field outside the stripes. In spite of the fact that the electric field is constant here, the detuning decreases for larger oscillation amplitudes as the integrated effect of the electron field gets smaller compared with the natural betatron motion. An analytic approximation of the detuning, valid for  $X \gg R_1$  is (see Appendix)

$$\Delta Q_{x,ec1,o}(I_x) = \frac{4 R_1 \Delta Q_{x,ec1}}{\pi \sqrt{2\beta_{x,IP} I_x}}. \quad (3)$$

In Fig. 2a we compare results from Eq. (3) with numerical evaluations of the tune and find an excellent agreement.

The situation can be more complicated if the test particle has a small or moderate oscillation amplitude and is located at a longitudinal position in the bunch where  $R_1 > \Delta R$ . In this case for a particle with a maximum amplitude  $X < R_1 - \Delta R$ , the tune will equal the unperturbed betatron tune as no electron force is present on the inner side of the electron stripe. If  $X > R_1$  the particle will spend part of its time outside the stripe, and part of it inside. Therefore the resulting detuning will be somewhat reduced with respect to the case where  $X \approx R_1$  (e.g. see Fig. 2a). However, for  $X \gg R_1$  the particle will stay mostly outside the stripe, and therefore the detuning will approach the prediction of Eq. (3) where we substitute  $R_1$  with  $\Delta R$ . We can recognize this effect in Fig. 2b, where at large amplitudes the analytic curve (red) converges towards the numerical one (black). The green area represents the region of the stripe which at  $z = -0.4\sigma_z$  is located between 1 and  $2\sigma_x$  [and between  $-2$  and  $-1\sigma_x$ ]. If the test

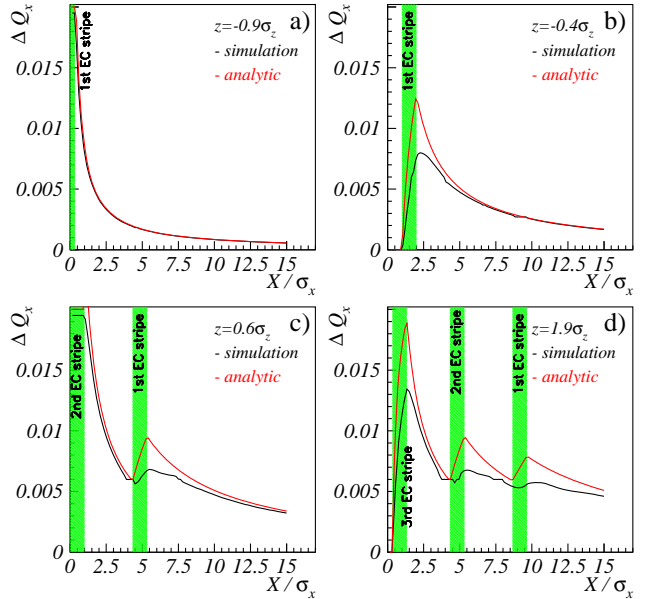


Figure 2: Detuning induced by the electron stripe model of Fig. 1 at several longitudinal positions along the bunch.

particle is situated at a longitudinal position and has a transverse amplitude such that two stripes are intercepted in the course of its oscillation the resulting detuning is the composition of the detuning induced by each of the two stripes (see Fig. 2c). In Fig. 2d at  $z = 1.9\sigma_z$  all three stripes are present. The overall effect is a significant residual detuning at large transverse amplitude ( $X = 15\sigma_x$ ) whereas the latter was practically zero at the pinch location of the first stripe (Fig. 2a). These numerical examples allow us to conclude that:

- The presence of electron stripes creates a detuning proportional to  $1/\sqrt{I_x}$  at large amplitudes.
- The varying horizontal position (or the ‘slope’) of the stripes introduces a  $z$ -dependence of the detuning with transverse amplitude which is analogous to the dependence of the detuning produced by space charge in high intensity bunches [30].
- The presence of multiple stripes creates a complex dependence of the detuning on the coordinates ( $z, x$ ) and it reduces the decrease of the electron-cloud induced detuning with transverse amplitude.

## PARTICLE DYNAMICS IN PRESENCE OF ELECTRON CLOUD STRIPES

We here discuss the single particle dynamics in presence of 1-dimensional electron stripes at a single IP (modeled as in Fig. 1). Our example accelerator is described by a smooth approximation, and we assume the typical tunes of the SPS:  $Q_x = 26.185$ , and  $Q_y = 26.136$ . For the sake of example, we select an electron density  $\rho_e$  which gives rise to an electron detuning of  $\Delta Q_{x,ec1} = 0.1$ . The presence of a single IP excites all resonances whose driving terms are present in the electron-induced force. On this occasion we note that the electron force is constant everywhere but within the stripe, and represents a strong nonlinearity which excites all harmonics. The dynamical properties of this system are better understood by studying the Poincaré sections of the frozen system, i.e. without synchrotron motion. We take the start particles at  $z = -0.9\sigma_z$ , i.e. at the location of the first pinch. In Fig. 3a the presence of 5 filled islands and 5 empty ones suggest that a 10th order resonance is excited by 1 IP. In Fig. 3b we show the beam particle detuning as a function of the particle amplitude  $X$ . The presence of islands is detected by the flat region in the tune curve. When we launch the test particles at a different longitudinal position, for example at  $z = -0.6\sigma_z$  see Fig. 3c, the 5 occupied islands are located further outward than in Fig. 3a. This is reminiscent of what happens for bunched beams that are space-charge dominated. However, the reason why the islands move outward is different: In high intensity bunches dominated by space charge the islands are located outward for small  $|z|$  because the space charge is larger close to the bunch center, hence the detuning increases at the center. In the present example instead,

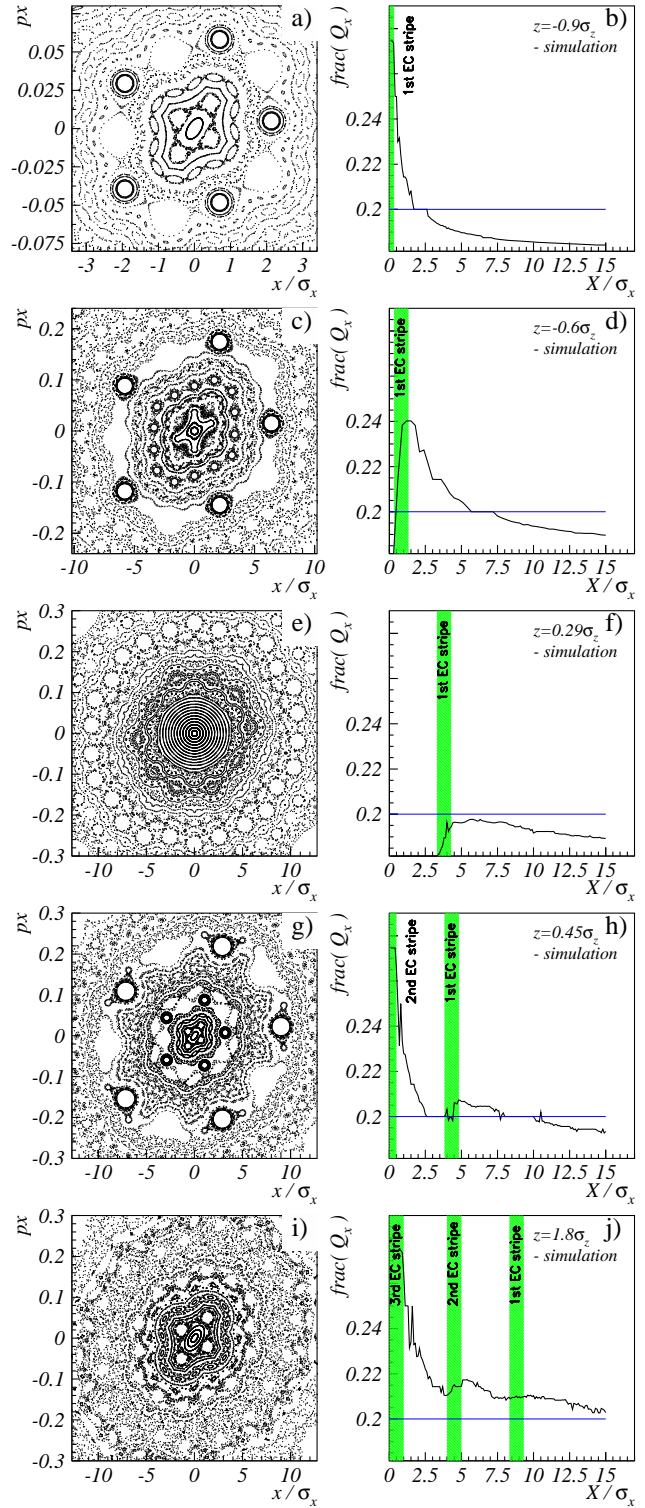


Figure 3: Transverse phase space (left) and nonlinear tune (right) for test particles at several transverse and longitudinal locations.

at  $z = -0.6\sigma_z$ , the electron stripes are located further outward (at  $x = 1.33\sigma_x$ ) than for  $z = -0.9\sigma_z$ , but since there now are more electrons inside the stripe (which builds up from  $z = -1.0\sigma_z$  to  $z = -0.7\sigma_z$ ) the net result is an increase in the detuning. This is visible in Fig. 2a where  $\Delta Q_{x,ec} = 1.67 \times 10^{-3}$ , at  $X = 5\sigma_x$  while in Fig. 2b at  $X = 5\sigma_x$  the detuning is  $\Delta Q_{x,ec} = 4.74 \times 10^{-3}$ . The increased electron detuning pushes the islands outward, but when the stripes are far from the origin, and for particle amplitudes close to the stripes the increase of the detuning is compensated by the increase of the area inside the stripes. Globally this compensation leads to a decrease of the detuning which can be seen in Fig. 3f, where at  $X = 5\sigma_x$  the detuning is smaller than in Fig. 3d. Note that in this last case (Fig. 3f), the tunes of the test particles stay below the 10th order resonance, and therefore 10th order islands no longer appear in phase space. Also visible in Fig. 3e is a peculiarity of our model in which electron forces are absent inside the electron stripes, namely that the inner region of the phase space here exhibits completely unperturbed Courant-Snyder ellipses. When the second electron stripe emerges, at  $z = 0.45\sigma_z$  (Figs. 3g,h), the detuning is strongly enhanced close to the origin, and more weakly increased further away, but the overall effect is that the test particle tune crosses the 5th order resonance at two positions, namely at  $X = 3.5\sigma_x$  and at  $X = 9\sigma_x$ . This is reflected in Fig. 3g by the presence of two chains of five islands. This additive effect of the electron stripes on the detuning is found at all longitudinal positions. In particular, at  $z = 1.8\sigma_z$  we observe that the tunes  $\Delta Q_{x,ec}$  always lie above the 5th order resonance for all values of  $X$  and therefore no 10th or 5th order island is found (see Figs. 3i,j). In other words, for intense bunched beams, the electron stripes introduce an  $x - z$  correlation in the position of the transverse islands, which are self generated and strongly excited due to the concentration of electrons at a single interaction point.

## TRAPPING ON RESONANCE CROSSING

In the previous section we uncovered several analogies between the pinched electron cloud and space-charge effects for intense bunched beams. We now explore if a shift of the tune across the 10th order resonance may induce particle trapping in the presence of an electron pinch as is the case for space charge. There is one important difference: For space-charge dominated intense bunched beams, the resonance is normally excited by a nonlinear driving term of the optical lattice, whereas in the case of the electron pinch the resonance driving term is provided by the electron stripes themselves. In the simulation, we first induce a resonance crossing by varying the accelerator tune  $Q_{x,0}$  over  $10^4$  turns from 26.185 to 26.22, so that we intersect the resonance  $10Q_x = 262$ . We launch a test beam particle of initial coordinates  $x = 2\sigma_x$ ,  $z = -0.95\sigma_z$ , and  $p_x = p_z = 0$  so that only the effect of the 1st stripe is included. Then we simulate the resonance crossing, keep-

ing the synchrotron motion of our particle frozen. Here the speed of the crossing is intentionally chosen to be much smaller than what it might be for a real bunched beam, as the trapping is facilitated if adiabatic conditions are met. The electron density of the stripe is adjusted via Eq. (3) so that it creates a detuning of  $\Delta Q_{x,ec1} = 0.1$ . In Figs. 4a,b

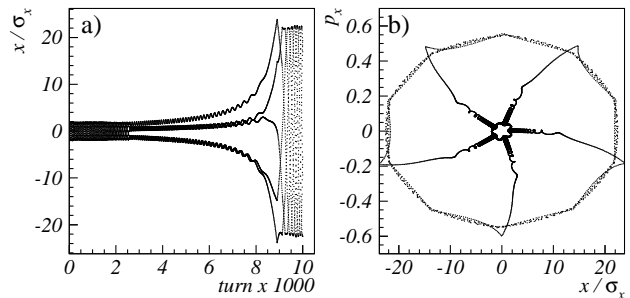


Figure 4: Crossing of the 10th order resonance by varying  $Q_{x,0}$ .

we show the particle amplitude versus the number of turns. The trapping is evident. Note that the particle is escaping towards infinity very fast when the tune is on the resonance, and finally a de-trapping takes place leaving the particle at a very large transverse amplitude, in this example at  $X \approx 20\sigma_x$ . This result strongly depends on the speed of the resonance crossing: the slower the crossing the larger is the amplitude gain, consistent with the theory of Schoch [1]. This dependence is similar to what was shown in Refs. [31, 32, 33] for high-intensity bunched beams with space charge. Figure 5 presents a detail of the trapping with a typical spiraling of the particle in phase space, following the outward moving islands.

The second fundamental type of resonance crossing occurs when the bare tune  $Q_{x,0}$  is fixed, but the particle is allowed to longitudinally oscillate according to the synchrotron motion. The dynamics of this case is much more complex as the particles travel through different longitudinal sections of the bunch for which the electron stripes vary in number and position. As a first step to approach this problem we consider the single passage through a resonance over half a synchrotron oscillation. We set the synchrotron period equal to  $2 \times 10^4$  turns and take a test particle located at the head of the bunch with initial coordinates:  $x = 2\sigma_x$ ,  $z = -3\sigma_z$ ,  $p_x = p_z = 0$ . The density of the electron-cloud is again adopted to produce a detuning of  $\Delta Q_{x,ec1} = 0.1$  at the pinch location. The tunes of the ring are those of the SPS:  $Q_{x,0} = 26.185$ ,  $Q_{y,0} = 26.136$ . In Fig. 6a we present the motion of the test particle in the  $x - z$  plane. The motion appears to be regular until  $z \approx -1\sigma_z$  is reached, where the first electron stripe is encountered. Following this, the motion ceases to be regular, but trapping does not yet occur as the important islands are still well inside the particle orbit. An island trapping takes place only at  $z \simeq -0.35\sigma_z$ . The trapping is evidenced in Fig. 6b by the 5 arms leaving the inner,

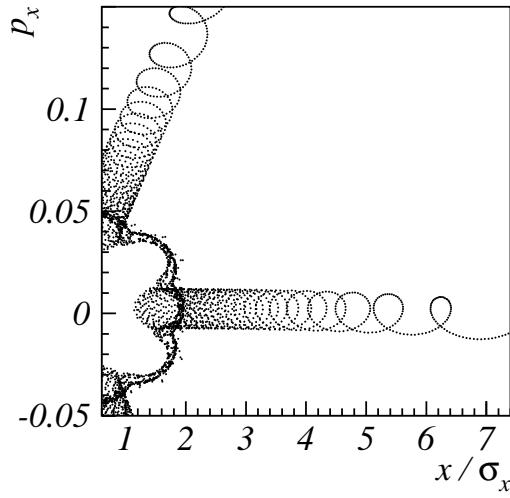


Figure 5: Detail of Fig. 4b: particle trapping induced by electron-cloud stripes.

smaller deformed ellipse. Also, due to a stroboscopic effect, the same trapping is signaled by 3 arms in Fig. 6a. A de-trapping occurs at  $z \simeq 0.1\sigma_z$ , from when on the islands no longer intercept the particle orbit. In particular the resonance is not crossed anymore by our particle in the region  $z = [0.15, \dots, 0.25]\sigma_z$ , whereas in the following interval  $z = [0.25, \dots, 0.3]\sigma_z$  the islands disappear entirely and the particle executes a nearly regular betatron motion. Both these effects are visible in Fig. 6a, where the three arms vanish. Then, islands are newly formed at  $z \geq 0.3\sigma_z$ , namely two or three chains of 10th order islands (see Fig. 3g). Our tracked particle is located between the inner and outer island chains. The outer chain does not intercept the particle orbit, while the inner smaller chain of islands never succeeds in crossing the particle orbit: for  $z > 0.46\sigma_z$  the detuning is already so large that the particle tune is moved above the 10th order resonance. Consequently in the region  $z = [0.4, \dots, 1.2]\sigma_z$ , the particle mainly undergoes chaotic betatron-like motion. Note, however, that the further outward the electron stripes are located, the weaker becomes the electron-induced detuning. At  $z \simeq 1\sigma_z$  the reduction of the detuning is such that the test particle again assumes a tune on the 10th order resonance. A “trapping” now takes place (see the stroboscopic effect in  $1.2\sigma_z < z \lesssim 1.5\sigma_z$ ). When the third electron stripe commences, at  $z = 1.5\sigma_z$ , the detuning rises again, eliminating all 10th order islands. This is visible in Fig. 6a by the irregular motion in the interval  $1.5\sigma_z < z < 2.3\sigma_z$ . For  $z > 2.3\sigma_z$  the electron-induced detuning shrinks again and the 10th order islands reappear, but no full trapping takes place. The partial trapping of this phase is visible by a weak signature of some stroboscopic effect in Fig. 6a, in

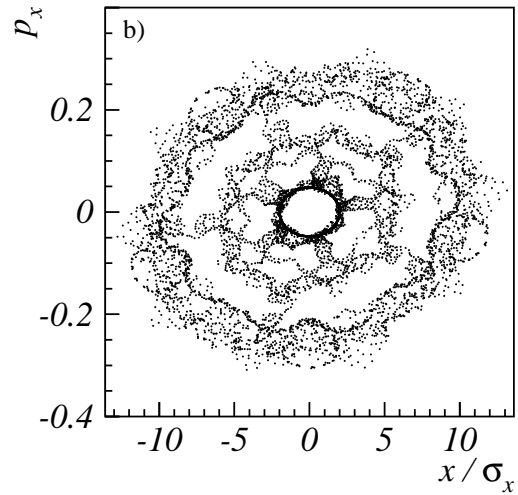
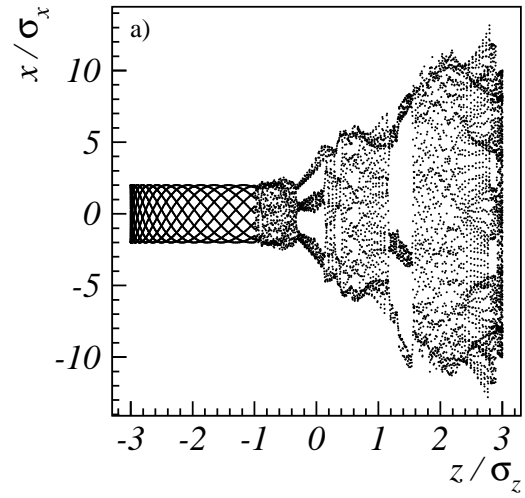


Figure 6: Crossing of the 10th order resonance in half a synchrotron period.

the region  $2.3\sigma_z < z < 3\sigma_z$ . This last part of the particle’s motion corresponds to the outer halo in Fig. 6b.

## EXAMPLE APPLICATIONS

The aim of the previous section was to demonstrate that trapping by electron stripes is possible. However, in normal operating conditions, most synchrotrons work in the “non adiabatic” regime, with longitudinal oscillations much faster than in the previous examples. The fast longitudinal oscillations create a complicated dynamical situation, where resonance trapping is dominated by “scattering” [34] (see also the original discussion of fast resonance crossing by Schoch [1]). We now apply our toy model for

the electron stripes described in Fig. 1 to the SPS ring assuming a realistic longitudinal frequency  $Q_{z,0} = 1/168$ . Figure 7a presents the simulated emittance growth for 120 electron-cloud interactions equally distributed around the SPS ring. In Fig. 7b there are 744 electron-cloud interactions, one for each dipole according to the SPS structure. The total electron-induced detuning is again chosen equal to 0.1. Note the asymmetric response of the beam growth for a swapping of the horizontal and vertical tunes as a consequence of the crossing or non crossing of the 10th order resonance. In spite of the different number of interactions, the beam response is comparable in the two pictures. In Fig. 7b the emittance growth is slightly smaller than in Fig. 7a as the smaller number of interaction points excites the 10th order resonance more strongly. In all these simulations we assumed a zero chromaticity, a linear lattice, and an accelerator optics modelled in smooth approximation.

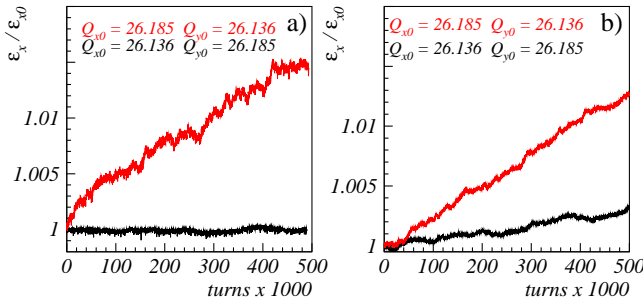


Figure 7: Example application to the SPS: a) electron IPs uniformly distributed around the circumference; b) one electron IP for each of the 744 dipoles in the SPS lattice.

We also applied this modeling of electron stripes to the future SIS100 ring at the GSI, even though the occurrence of an electron cloud at SIS100 is not yet fully assessed [35]. Figure 8a shows the simulated emittance growth during  $120 \times 10^3$  turns, and Fig. 8b the accompanying halo development. The working points are  $Q_{x,0} = 18.84$ ,  $Q_{y,0} = 18.73$ , and the longitudinal tune is  $Q_{z,0} = 10^{-3}$ . A more detailed discussion of the SIS100 parameters and the associated space-charge issues can be found in Ref. [36]. The results of our simulation show an emittance increase by 12%, and the fraction of halo particles outside  $3\sigma_x$  exceeding 2%. Though these results appear acceptable compared with the beam-loss budget, a complete evaluation of the actual electron-cloud density expected in SIS100 still remains to be carried out.

## CONCLUSION

The study presented in this report demonstrates that the morphological fine structure of the electron-cloud pinch plays an important role in creating the amplitude dependent detuning responsible for island migration and consequent particle trapping. Differently from the space-charge induced resonance trapping, the multiple stripes formed by

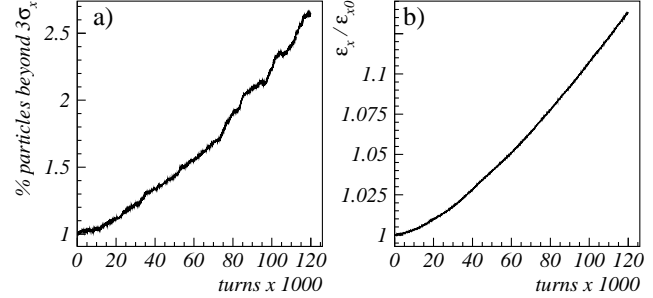


Figure 8: Application of the one dimensional electron stripe model to SIS100. a) emittance increase; b) % of particles beyond  $3\sigma_x$ . In this simulations the total electron-induced detuning is chosen equal to 0.1.

the electron cloud induce multiple resonance crossings due to slow synchrotron motion. The complexity of the dynamics is fully illustrated by Fig. 6 where in half a synchrotron period the trapping and diffusion regimes alternate several times. We expect that a refined modeling of the electron stripes will create an even more complex dynamics which renders the reliable prediction of long term emittance growth a challenging endeavour indeed.

## ACKNOWLEDGMENT

We acknowledge the support of the European Community-Research Infrastructure Initiative under the FP6 ‘‘Structuring the European Research Area’’ programme (CARE, contract number RII3-CT-2003-506395).

## APPENDIX

The detuning created by one localized EC kick can be computed as follows. Consider the beam-particle motion in a section of the storage ring where the beam-electron interaction is located. In this section let the beta function be  $\beta_{x,IP}$ , and for simplicity adopt a smooth approximation with  $\alpha_{x,IP} \approx 0$ . In Courant-Snyder variables the particle’s phase-space coordinates then are  $\hat{x} = \sqrt{2I_x} \cos(\theta_x)$ , and  $\hat{x}' = \sqrt{2I_x} \sin(\theta_x)$ , with  $\theta_x$  denoting the betatron phase of the particle and  $I_x$  the classical action variable. The average shift in the betatron phase advance after  $N$  turns, due to the additional deflections  $\Delta x'_i$  ( $i = 1, \dots, N$ ) experienced at a single beam-electron interaction point on successive turns, is

$$\Delta\theta_x = \frac{1}{N} \sum_{i=1}^N \frac{\sqrt{\beta_{x,IP}} \Delta x'_i \cos(\theta_{x,i})}{\sqrt{2I_x}}, \quad (4)$$

where  $\theta_{x,i}$  denotes the betatron phase on turn  $i$ . In Eq. (4) we assume that the invariant  $I_x$  remains constant, i.e. we exclude any resonant effect, or, in other words, we are averaging over a number of turns  $N$  sufficiently small that the growth of  $I_x$  is negligible, but large enough for phase averages to make sense. For applying Eq. (4) to the effect of

the pinched electrons, we first note that, in our toy model, the EC electric field  $E_x$  inside the emerging stripes close to the center of the pinch  $z_p$ , is given by

$$E_{ec,x} = -\frac{e\rho_e}{\epsilon_0}x. \quad (5)$$

Inserting the resulting deflection  $\Delta x'$ , which is also linear in the offset  $x$ , into Eq. (4) the calculation reduces to an average over the term  $\cos^2(\theta_{x,i})$  which can be estimated analytically using the aforementioned assumptions. We then find that one IP for a particle with small transverse amplitude will give rise to the detuning

$$\Delta Q_{x,ec1} = \frac{\beta_{x,IP}}{4\pi} \frac{e\rho_e}{\epsilon_0} \frac{q}{p_0 v_0} \Delta s. \quad (6)$$

We can therefore express the density of a stripe as a function of the EC detuning in the pinch as

$$\rho_e = \epsilon_0 \frac{4\pi}{\beta_{x,IP}} \frac{\Delta Q_{x,ec1}}{\Delta s} \frac{p_0 v_0}{eq}. \quad (7)$$

For a particle at large transverse amplitude with respect to the stripe location  $R_1 > \Delta R$ , we can approximate the electron field as

$$E_{x,o} = -\frac{e\rho_e}{\epsilon_0} \Delta R \text{sign}(\hat{x}). \quad (8)$$

and again apply Eq. (4). In the expression (8) we do not distinguish between the inside of the stripe (where  $E_x = 0$ ) and the outside (where the field is constant) because, for large betatron amplitudes, the inside of the stripe occupies only a small fraction of the area spanned by the particle motion, which will not significantly contribute to the overall detuning. By combining Eq. (8) and Eq. (4) the detuning at large amplitudes becomes

$$\Delta Q_{x,ec1,o} = \frac{1}{\pi^2} \sqrt{\beta_{x,IP}} \left( \frac{e\rho_e}{\epsilon_0} \frac{q}{p_0 v_0} \Delta s \right) \frac{\Delta R}{\sqrt{2I_x}}, \quad (9)$$

and inserting  $\rho_e$  from Eq. (7) we finally obtain the equation for the tune shift. Note that if  $0 < R_1 < \Delta R$  then we substitute  $\Delta R$  with  $R_1$  and obtain Eq. (3).

## REFERENCES

[1] A. Schoch, "Theory of Linear and Non-Linear Perturbations of Betatron Oscillations in Alternating Gradient Synchrotrons," CERN 57-21 (Proton Synchrotron Division), Section 14 (1958).  
[2] A. Chao and M. Month, "Particle Trapping during Passage Through a High-Order Nonlinear Resonance," Nuclear Instruments Methods **121**, p. 129 (1974).  
[3] B.V. Chirikov, M.A. Lieberman, D.L. Shepelyansky, F.M. Valdi, "A Theory of Modulational Diffusion," Physica D, **14**, 3, 289–304 (1985).  
[4] L.R. Evans, "The Beam-Beam Interaction," CERN Accelerator School 'Antiprotons for Colliding Beam Facilities', CERN October 1983, CERN **84-15**, p. 319 (1984).

[5] F. Zimmermann, "Transverse Proton Diffusion," Particle Accelerators **49**, 67–104 (1995).  
[6] M. Giovannozzi, W. Scandale, E. Todesco, "Dynamic Aperture Extrapolation in the Presence of Tune Modulation," Phys. Rev. E **57**, 3432–3443 (1997).  
[7] F. Ruggiero, F. Zimmermann, "Consequences of the Direct Space Charge Effect for Dynamic Aperture and Tail Formation in the LHC," PAC'99 New York, vol. **4**, 2626 (1999).  
[8] M.A. Furman and A.A. Zholents, "Incoherent Effects driven by the Electron Cloud," PAC 99 New York, Vol. **3**, 1794 (1999).  
[9] K. Ohmi and F. Zimmermann, "Head-Tail Instability Caused by Electron Cloud in Positron Storage Rings," Phys. Rev. Letters **85**, 3821 (2000).  
[10] J. Flanagan *et al.*, "Observation of Vertical Betatron Sideband due to Electron Clouds in the KEKB LER," Phys. Rev. Letters **94**:054801 (2005).  
[11] H. Fukuma *et al.*, "Study of Vertical Beam Blowup in KEKB Low Energy Ring," Proc. HEACC 2001 Tsukuba <http://conference.kek.jp/heacc2001/>  
[12] F. Zimmermann, H. Fukuma, K. Ohmi, CERN-SL-Note-2000-061, November 2000.  
[13] F. Zimmermann, "Electron Cloud Simulations: An Update," Proc. Chamomix XI, p. 144, CERN-SL-2001-003-DI (2001).  
[14] G. Rumolo, F. Zimmermann, "Electron-Cloud Instability with Space Charge or Beam Beam", 3rd paper in 'Contributions of the SL-AP Group to the Two-Stream Instabilities Workshop,' CERN-SL-2001-067 (2001).  
[15] K. Ohmi, "Single Bunch Electron Cloud Instability for a Round Beam," Memorandum, November 2002; see <http://ab-abp-rlc-ecloud.web.cern.ch/ab-abp-rlc-ecloud>  
[16] K. Ohmi, "Single Bunch Electron Cloud Instability for a Round Beam II," Memorandum, December 2002, see <http://ab-abp-rlc-ecloud.web.cern.ch/ab-abp-rlc-ecloud>  
[17] E. Benedetto *et al.*, "Transverse 'Monopole' Instability driven by Electron Cloud?," PAC 2003, Portland (2003).  
[18] E. Benedetto and F. Zimmermann, "Analysis of the Electron Pinch during a Bunch Passage," Proceedings ELOUD'04, Napa April 2004, CERN Report CERN-2005-001, p. 81 (2005).  
[19] E. Benedetto and F. Zimmermann, "Dynamics of the Electron Pinch and Incoherent Tune Shift Induced by Electron Cloud," Proc. of EPAC'04, Lucerne, Switzerland, WE-PLT009, p. 1834 (2004).  
[20] D. Kraemer, Proc. EPAC 2007, THXAB02, p. 2598; P. Spiller, Proc. HB2006 ICFA Workshop, Tsukuba, Japan, 29 May – 2 June 2006, MOBP02, p. 24.  
[21] G. Franchetti *et al.*, Phys. Rev. ST Accel. Beams **6**, 124201 (2003); E. Metral *et al.*, NIM A **561**, 257 (2006).  
[22] G. Franchetti, I. Hofmann, Proc. HB2006 ICFA Workshop, Tsukuba, Japan 29 May - 2 June 2006, WEAX01, p. 167; ed. H. Sako (2006).  
[23] E. Metral, E. Shaposhnikova, G. Arduini, private communication (2006).  
[24] E. Benedetto *et al.*, "Emittance growth caused by electron cloud below the "fast TMCI" threshold: numerical noise or true physics?," PAC2005 Knoxville, USA, p. 1344 (2005).



- [25] E. Benedetto, G. Franchetti, F. Zimmermann, Phys. Rev. Lett., **97**, 034801 (2006).
- [26] K. Ohmi, K. Oide, "Chaos and Emittance Growth due to Nonlinear Interactions in a Circular Accelerator," Phys. Rev. ST Accel. Beams **10**:014401 (2007).
- [27] G. Rumolo, F. Zimmermann "Practical User Guide for HEADTAIL," SL-Note-2002-036-AP (2002).
- [28] E. Benedetto, "Emittance Growth Induced by Electron Cloud in Proton Storage Rings," PhD Thesis Politecnico di Torino (2006).
- [29] E. Benedetto *et al.*, "Modeling Incoherent Electron-Cloud Effects," Proc. of PAC'07, Albuquerque, New Mexico, USA. THPAN075, p. 3393 (2007).
- [30] G. Franchetti *et al.*, "Long-Term Simulations of Space Charge and Beam Loss Observed in the CERN PS," Proc. ICFA Workshop HB2004, Bensheim, Germany 18-22 October 2004, eds. I. Hofmann, J.-M. Lagniel, and R.W. Hasse, AIP **773**, 137 (2004).
- [31] G. Franchetti, "Recent Developments in Understanding Beam Loss in High-Intensity Synchrotrons," Proc. of PAC'07, Albuquerque, New Mexico, USA. TUZAAB02, p. 794 (2007).
- [32] I. Hofmann and G. Franchetti, "Scaling Laws for Space-Charge Driven Resonances," Proc. of PAC'07, Albuquerque, New Mexico, USA. THPAN017, p. 3259 (2007).
- [33] S.Y. Lee *et al.*, New J. Phys. **8** (2006) 291; S.Y. Lee, Phys. Rev. Lett. **97**, 104801 (2006).
- [34] A.I. Neishtadt, "Scattering by Resonances," Celestial Mech. Dyn. Astronomy, vol. **65**, p. 1-20 (1997).
- [35] G. Rumolo and O. Boine-Frankenheim, "Study of Electron Cloud Formation and Instability in SIS," Internal note, GSI-Acc-Note-2003-10-001, (2003).
- [36] G. Franchetti *et al.*, "Space charge and electron clouds issues", Proc. of LHC Lumi 2006, October 16-20 2006, Valencia, Spain. p. 192 (2006).